Plant Physiology and Biochemistry 49 (2011) 520–529

Contents lists available at ScienceDirect

Plant Physiology and Biochemistry

journal homepage: www.elsevier.com/locate/plaphy

Research article

Identification of an *Arabidopsis* mitoferrinlike carrier protein involved in Fe metabolism

Delia Tarantino [a], Piero Morandini [a], Leonor Ramirez [a,b], Carlo Soave [a], Irene Murgia [a,*]

[a] Sezione di Fisiologia e Biochimica delle Piante, Dipartimento di Biologia, Università degli Studi di Milano, via Celoria 26, 20133 Italy
[b] Instituto de Investigaciones Biologicas, Universidad Nacional de Mar del Plata, CC 1245, 7600 Mar del Plata, Argentina

ARTICLE INFO

Article history:
Received 12 October 2010
Accepted 3 February 2011
Available online 12 February 2011

Keywords:
Arabidopsis
Carriers
Chloroplasts
Correlation analysis
Iron
Mitochondria
Mitoferrin

ABSTRACT

Iron has a major role in mitochondrial as well as in chloroplast metabolism, however the processes involved in organelle iron transport in plants are only partially understood.

To identify mitochondrial iron transporters in *Arabidopsis*, we searched for proteins homologous to the *Danio rerio* (zebrafish) Mitoferrin2 MFRN2, a mitochondrial iron importer in non-erythroid cells. Among the identified putative *Arabidopsis* mitoferrinlike proteins, we focused on that one encoded by At5g42130, which we named *AtMfl1* (MitoFerrinLike1).

AtMfl1 expression strongly correlates with genes coding for proteins involved in chloroplast metabolism. Such an unexpected result is supported by the identification by different research groups, of the protein encoded by At5g42130 and of its homologs from various plant species in the inner chloroplastic envelope membrane proteome. Notably, neither the protein encoded by At5g42130 nor its homologs from other plant species have been identified in the mitochondrial proteome.

AtMfl1 gene expression is dependent on Fe supply: *AtMfl1* transcript strongly accumulates under Fe excess, moderately under Fe sufficiency and weakly under Fe deficiency.

In order to understand the physiological role of *AtMfl1*, we isolated and characterized two independent *AtMfl1* KO mutants, *atmfl1-1* and *atmfl1-2*: both show reduced vegetative growth. When grown under conditions of Fe excess, *atmfl1-1* and *atmfl1-2* mutants (seedlings, rosette leaves) contain less total Fe than wt and also reduced expression of the iron storage ferritin *AtFer1*.

Taken together, these results suggest that *Arabidopsis* mitoferrinlike gene *AtMfl1* is involved in Fe transport into chloroplasts, under different conditions of Fe supply and that suppression of its expression alters plant Fe accumulation in various developmental stages.

1. Introduction

Fe is an essential element for all living organisms [1]; the eukaryotic subcellular compartmentalization poses the question of the mechanisms facilitating Fe transport into such organelles, the regulation of their Fe homeostasis and Fe trafficking in such compartments.

In plant cells the synthesis of heme and [Fe–S] clusters, two different co-factors required for proper functionality of many different Fe-containing enzymes, takes place in both chloroplasts and mitochondria, though with different pathways for the [Fe–S] cluster [2]. Heme, like all tetrapyrroles, is synthesised in chloroplasts but evidence for the occurrence of the last three steps of heme biosynthesis in mitochondria has been reported [3–6].

Demand for Fe in both organelles is therefore high and indeed around 90% of Fe in leaf cells is located in chloroplasts, with 75–80% in the chloroplastic stroma [7]; however, mechanisms of Fe transport to chloroplasts and mitochondria have just begun to be elucidated.

At2g15290 encodes an *Arabidopsis* protein essential for plants; this protein, named either PIC1 (Permease in Chloroplasts) [8] or TIC21 (Translocon at the Inner envelope membrane of Chloroplasts) [9,10] is localized in the inner envelope of chloroplasts [8,9]. *Arabidopsis pic1* KO mutants grow only heterotrophically and show a dwarfish and chlorotic phenotype [8]. PIC1 and its homolog from *Synechocystis* mediate iron uptake in yeast double mutant *fet3fet4*, which is defective in Fe uptake [8]; also, accumulation of ferritin clusters occurs in *pic1* chloroplasts, leading to the hypothesis that PIC1 functions in Fe transport across that membrane [8]. However,

Abbreviations: AIS, Arabidopsis growth medium; Col, Columbia; DW, dry weight; EDTA, ethylenediaminetetracetic acid; KO, knock out; EDDHA, ethylenediamine-*N*,*N*′-bis(2-hydroxyphenylacetic acid); FW, fresh weight; SE, standard error; T-DNA, transferred DNA; WT, wild-type.

* Corresponding author. Tel.: +39 02 50314837; fax: +39 02 50314815.
E-mail address: irene.murgia@unimi.it (I. Murgia).

0981-9428/$ – see front matter © 2011 Elsevier Masson SAS. All rights reserved.
doi:10.1016/j.plaphy.2011.02.003

conflicting results on the role of PIC1 have been reported: total iron content in *pic1* leaves is not altered, when compared to wt [8] and PIC1 expression is not regulated by Fe. In fact, other research groups showed that At2g15290 encodes a component of a translocation complex which mediates chloroplast protein import across the inner envelope membrane, which has been named TIC21 [9,10]. Such hypothesis is supported also by the evidence that *tic21* (alias *pic1*) mutants are defective in the import of photosynthetic proteins.

Dicots and non graminaceous monocots absorb Fe from the soil by a three-step strategy I: solubilization of Fe(III) through acidification by H^+-ATPase activity, reduction of Fe(III) to Fe(II) by Ferric chelate reductases and Fe(II) uptake by Iron Root Transporters [1,11–13]. Fe(III) has a very low solubility at neutral pH in the presence of oxygen, and an alternative to Fe(III) reduction to Fe(II) is direct chelation of Fe(III) from the soil though phytosiderophores, as it occurs in graminaceous monocots [1,12–14]. Ferric chelate reductase FRO2 is responsible for reduction of iron at the root surface [11,12] but also other members of the FRO family reduce ferric Fe (III) chelates to form soluble Fe(II) [13]. Some FROs isoforms are localized on organellar membranes, such as the chloroplast FRO7, which contributes to the chloroplast Fe acquisition [15].

FRO isoforms are also located in mitochondria, such as FRO3 and FRO8 [12]. FRO3 expression levels are much higher in *Arabidopsis atfer4* mutants whose mitochondrial Fe content is higher than wt [16]. FRO3 expression is induced by Fe deficiency [11] and exposure to Fe excess reduces its expression in *atfer4* cells [16]. FRO8 is not regulated by Fe availability [11] and it is not expressed in *atfer4* cells [16], thus suggesting that FRO3 and FRO8 play different roles in mitochondrial Fe transport.

AtATM3 (alias STA1), an ATP-binding cassette mitochondrial transporter of *Arabidopsis*, is essential for Fe homeostasis and it is implicated in heavy metal resistance [17,18]. Experimental evidence suggests that AtATM3 has a role in transporting [Fe–S] clusters and in regulating cellular GSH levels, possibly by transporting GS-conjugated Cd (II) and/or [Fe–S] clusters across the mitochondrial membrane [18].

Current knowledge of mitochondrial Fe uptake in vertebrate cells can assist the search for Fe transporters into plant mitochondria, in particular *Danio rerio* (zebrafish) is a model used to study different heritable and hematological disorders in humans. Cloning of the *D. rerio frs* locus, associated with severe anaemia and paucity of mature erythrocites cells, allowed the identification of a member of the SLC25 carrier family, expressed in the inner mitochondrial membrane of eukaryotes; this gene mutated in *frs* mutants was therefore named mitoferrin1 *Mfrn1* [19]. Subsequently, a second mitoferrin was also identified, named mitoferrin2 (*Mfrn2*) [19], also localized in mitochondria [20]. *Mfrn1* and *Mfrn2* expression pattern was investigated in different cell lines, as well as mitochondrial iron assimilation in different Mfrn-deficient cell lines (erythroid and non-erythroid) and the effects of *Mfrn1* and *Mfrn2* ectopic expression [19,20]. Results indicate that both MFRN1 and MFRN2 are involved in Fe (II) assimilation into mitochondria and that they contribute to mitochondrial iron metabolism, because heme synthesis is severely reduced when both MFRNs are absent in non-erythroid cells. Although MFRN1 and MFRN2 are functionally redundant in non-erythroid cells, MFRN2 transports more iron into mitochondria than MFRN1 in undifferentiated cells, whereas MFRN1 is the principal mitochondrial iron importer and therefore essential for heme biosynthesis in erythroid cells [19,20].

To identify candidate genes involved in iron transport into plant mitochondria, we searched for *Arabidopsis* proteins showing sequence homology with the *D. rerio* (zebrafish) MFRN2, with the assumption that the plant cell requirement for iron might be more similar to undifferentiated animal cells than to erythroid ones. Among the different mitoferrinlike candidates identified so far, we focused on the *Arabidopsis* MitoFerrinLike1 *AtMfl1* gene At5g42130. We report in the present paper the analysis of its physiological role through the characterization of two independent *atmfl1* KO mutants.

2. Results

2.1. Arabidopsis gene At5g42130, named AtMfl1 (Mitoferrinlike1), encodes a protein belonging to the mitochondrial carrier family and similar to animal mitoferrin

To identify putative plant mitoferrins involved in mitochondrial Fe transport, a search of *Arabidopsis* candidate proteins homologous to MFRN2 was performed with BlastP program. The four *Arabidopsis* genes coding for proteins with highest sequence similarity with MFRN2 are the following (in brackets percent aminoacid identity): At1g07030 (37%), At2g30160 (36%), At1g34065 (30%), At5g42130 (27%), all members of the *Arabidopsis* mitochondrial carriers family [21] (Fig. 1). At1g07030 and At2g30160 were found to be duplicates residing in recent segment duplications between chromosome 1 and 2 [22] whereas At1g34065 codes for a protein named SAMC2 [23] since it has 62% amino acid sequence similarity with a plastid S-adenosylmethionine transporter [23,24], although its real physiological function is still unclear [25]. An un-rooted similarity tree of the various mitochondrial carrier family members, including At1g07030, At2g30160 and At5g42130 has been reported in [22].

Members of this family of carrier proteins are presumed to be targeted to the mitochondrial inner membrane [22]. Aramemnon is a plant membrane protein database which takes advantage of up to 17 individual programs for predicting subcellular location of a given protein (at http//aramemnon.botanik.uni-koeln.de). Aramemnon suggests in fact a chloroplast localization for the proteins encoded by At5g42130 and At1g34065 genes. According to ChloroP 1.1 (at http://www.cbs.dtu.dk/services/ChloroP/) which is one of the prediction programs used by Aramemnon, the chloroplast transit peptide (cTP) of the protein encoded by At5g42130 gene consists of its N-terminal 98 aa whereas the cTP of the protein encoded by At1g34065 gene consists of its N-terminal 43 aa.

No comments on the possible localization are provided by Aramemnon for proteins encoded by At1g07030 and At2g30160 genes.

To verify whether the genes listed in Fig. 1 can be genuinely attributed to the class of carrier proteins, the prediction of their transmembrane regions was also performed: according to TMpred all four encoded proteins have transmembrane domains: five transmembrane helices for At1g07030, At2g30160 and six predicted transmembrane helices for At5g42130 and At1g34065 (Fig. S1A). This latter prediction is consistent with the primary structure of six transmembrane α-helices described in an early study on non-plant mitochondrial carriers [26]. On the other hand, TMHMM Server v. 2.0 suggests three transmembrane domains (Fig. S1B) for At5g42130 and At1g34065.

Among these last two genes, we focused our analysis on *Arabidopsis* gene At5g42130, which we named *AtMfl1* (*MitoFerrinLike1*).

2.2. AtMfl1 expression correlates with the expression of genes involved in chloroplast metabolism and AtMFL1 protein is part of the chloroplast inner envelope membrane proteome

Correlation analysis has been recently applied for investigating gene function but also for identifying new candidate genes for specific processes [27–29]. The extent of correlation can be measured by the Pearson's correlation coefficient [30] using expression values as such or after logarithmic transformation. We have recently applied correlation analysis of a cytochrome P450

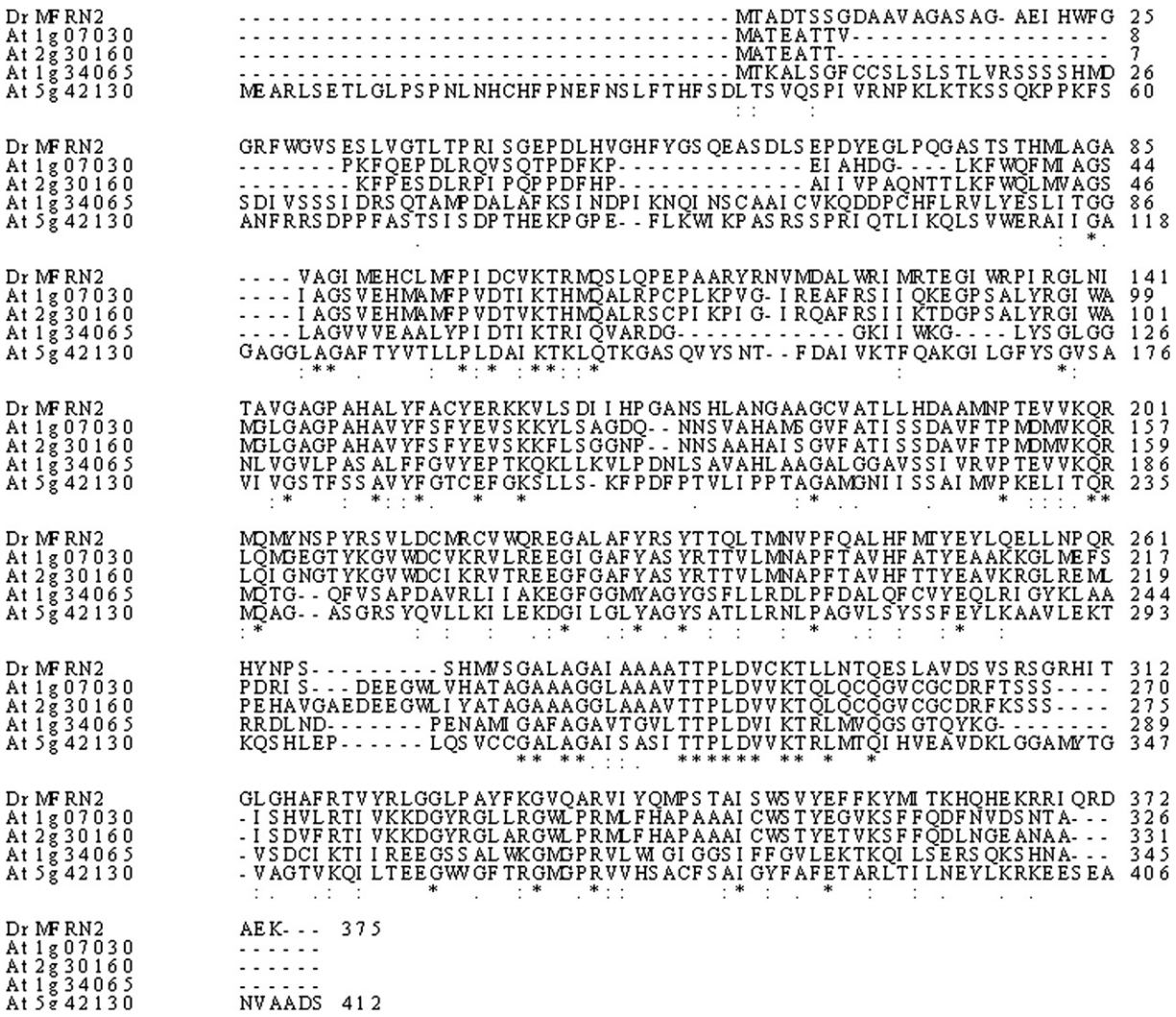

Fig. 1. Alignment of *Danio rerio* Mitoferrin2 MFRN2 with *Arabidopsis thaliana* mitochondrial carriers encoded by At1g07030, At2g30160, At1g34065, At5g42130 genes. The conserved aminoacids are indicated by *.

gene involved in the early Fe deficiency response [31]. In that study, we confirmed that correlation analysis can be more informative when in the log space, especially for genes with a tissue-, stage- or condition-specific expression.

Out of the top 35 genes with highest correlation with *AtMfl1*, 24 encode proteins annotated as chloroplastic whereas none of them encodes proteins which are solely mitochondrial (Table 1). Interestingly, correlation of *AtMfl1* with At2g15290 coding for the chloroplast PIC1/TIC21 is also high (0.7641) (Table S1).

These results prompted us to look for AtMFL1 protein in the database on subcellular proteomes publicly available. Although early proteome analyses on *Arabidopsis* did not report AtMFL1 in the group of identified chloroplast envelope proteins [32,33], AtMFL1 was later retrieved in the *Arabidopsis* inner chloroplastic envelope by mass spectrometry analysis [34–36] (see also Plant Proteomics Database at Cornell http://ppdb.tc.cornell.edu) whereas the other *Arabidopsis* mitoferrinlike proteins reported in Fig. 1 were not found as part of this proteome.

Also, homologs of AtMFL1 have been found in pea and maize chloroplast envelope membrane proteomes, by mass spectrometry analysis [37,38]; for both envelope proteome samples, the level of contamination from extraplastidial sources was very low (below 2.2% for maize and below 5.2% for pea) and no mitochondrial contamination was detected in maize chloroplast proteome. The identification of the AtMFL1 maize homolog in chloroplasts is therefore genuine, not a contamination artefact [37].

In agreement with these data, AtMFL1 was also found in the proplastid envelope membrane of *Brassica oleracea* ssp. *Botrytis* (cauliflower) [39], which is an excellent model for proteomics of meristematic tissues. A Mapman representation of the virtual plastid envelope displays Mitochondrial Carrier Family Proteins (MCF) in the inner chloroplastic envelope [39]. In accordance to these results, AtMFL1 was not retrieved in either stromal, thylakoidal or lumenal fractions of chloroplasts (e.g., [40]).

Most important, neither AtMFL1 nor the other mitoferrinlike proteins were found in the mitochondrial proteome analyses performed in [35,41] (see also http://www.genetik.uni-hannover.de/arabidopsis.html) strongly supporting the evidence that AtMFL1 retrieval in *Arabidopsis* chloroplasts could not be attributed to partial contamination of proteome samples with the mitochondrial fraction.

These results indicate that the *Arabidopsis* mitoferrinlike gene *AtMfl1* encodes a protein which could be specifically involved in chloroplast iron transport whereas the subcellular compartment in which the other mitoferrinlike proteins (Fig. 1) are active is not known yet.

Table 1
Arabidopsis genes with highest correlation values with *At5g42130* expression, according to logarithmic analysis. The genes are listed together with their respective Pearson's correlation coefficients, from log analysis. Genes coding for proteins annotated as solely chloroplastic are reported in bold, the ones coding for putative chloroplastic and/or mitochondrial proteins are reported in italics.

		Pearson's coeff. (log)
AT5G42130	MitoFerrinLike 1 MFL1	1
AT4G16390	**chloroplastic RNA binding protein P67**	0.838
AT3G12930	**expressed protein, of unknown function**	0.833
AT3G02450	**ATPase AAA family proten (ATPases associated with diverse cell activities)**	0.824
AT3G02660	*RNA binding tyrosine -tRNA ligase activity*	0.823
AT5G46580	**pentatricopeptide (PPR) repeat-containing protein**	0.817
AT1G03475	**coproporphyrinogen III oxidase**	0.814
AT2G03420	expresesd protein of unknown function	0.812
AT2G47590	photolyase/blue light photoreceptor (PHR2)	0.811
AT5G66470	**expressed protein /GTP binding/RNA binding**	0.811
AT5G11450	**oxygen-evolving complex-related**	0.809
AT5G55740	**pentatricopeptide (PPR) repeat-containing protein CRR21**	0.808
AT2G01290	Cytosolic ribose-5-phosphate isomerase RPI2	0.806
AT2G17033	pentatricopeptide (PPR) repeat-containing protein	0.804
AT2G25840	*tRNA synthetase*	0.802
AT3G28460	**expressed protein of unknown function**	0.802
AT3G52380	**RNA- binding protein cp33**	0.801
AT4G02990	mitochondrial transcription termination factor family protein	0.801
AT5G05740	**S2P-like putative metalloprotease**	0.800
AT1G74850	**pentatricopeptide (PPR) repeat-containing protein, regulation of transcription**	0.800
AT3G48730	**glutamate-1-semialdehyde aminotransferase2/ porphyrin biosynthesis**	0.800
AT4G39960	**DNAJ heat shock family protein**	0.798
AT4G20130	Plastid Transcriptionally active 14 (PTAC14)	0.798
AT1G02150	pentatricopeptide (PPR) repeat-containing protein	0.796
AT2G36990	**RNA polymerase sigma subunit SigF**	0.793
AT5G52010	**zinc finger (C2H2 type) family protein**	0.792
AT5G14460	**pseudouridylate synthase TruB family protein**	0.792
AT1G44920	expressed protein of unknown function	0.792
AT1G11430	**plastid developmental protein DAG**	0.792
AT1G07320	**plastid ribosomal protein L4**	0.791
AT3G03710	**chloroplast polyribonucleotide nucleotidyltransferase**	0.791
AT3G14930	**uroporphyrinogen decarboxylase**	0.790
AT3G10840	**hydrolase alpha/beta fold family protein**	0.790
AT3G25660	**glutamyl-tRNA (Gln) amidotransferase**	0.790
AT1G60600	**protein involved in plastoquinone biosynthesis**	0.789
AT2G33180	expressed protein of unknown function	0.788

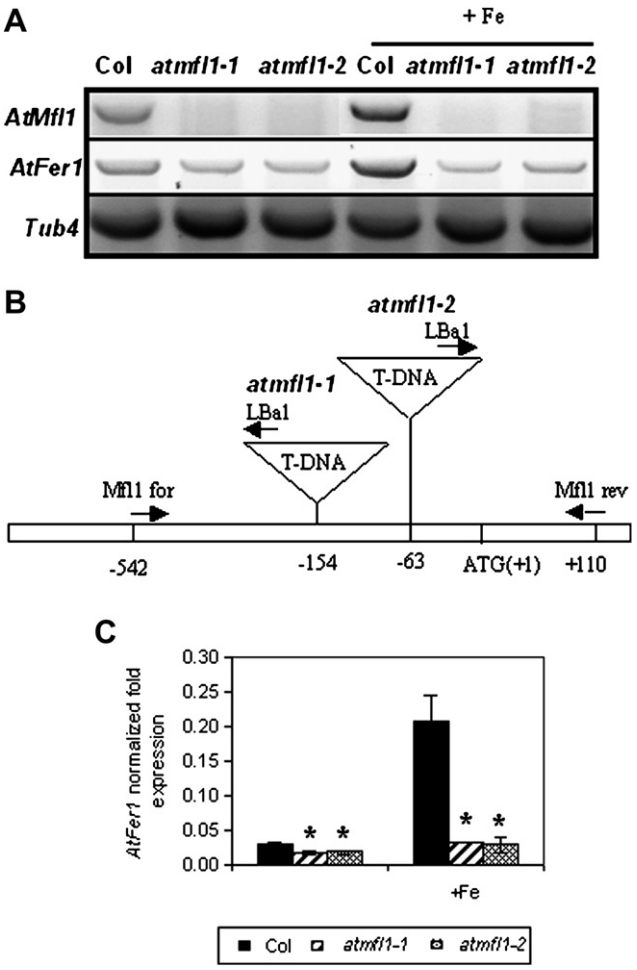

Fig. 2. T-DNA insertion in *atmfl1-1* and *atmfl1-2* KO mutants. (A) RT-PCR analysis of *AtMfl1* and *AtFer1* transcripts in rosette leaves of 21 d old wt Col, *atmfl1-1* and *atmfl1-2* plants, grown in control conditions or under constant, high Fe supplement (2.15 mM Fe (III) from Fe(III)-EDDHA). *Tub4* is the positive control, for testing the equal addition of RNA in each sample. (B) Diagram illustrates the site of the T-DNA insertions in *atmfl1-1* and in *atmfl1-2* mutants. Insertion points of the T-DNA in the promoter of the intronless *AtMfl1* gene (At5g42130) are indicated; arrows indicate the orientation of the primers; the diagram is not to scale. (C) Quantitative real-time RT-PCR on *AtFer1* transcript; the normalized fold expression was quantified in cDNA from 21 d old rosette leaves of wt Col, *atmfl1-1* and *atmfl1-2* plants, grown in control conditions or under constant, high Fe supplement (2.15 mM Fe(III) from Fe(III)-EDDHA). Bars represent mean values ± SE of three replicates.

2.3. Two independent AtMfl1 KO mutants atmfl1-1 and atmfl1-2 show reduced vegetative growth, reduced Fe content and reduced AtFer1 ferritin expression

AtMfl1 expression is mainly localized in rosette leaves and in developing flowers and siliques, according to *Arabidopsis* eFP Browser [42] (see also http://www.bbc.botany.utoronto.ca). RT-PCR analysis on rosette leaves of wt Col plants grown either in control condition or under constant Fe supplement confirms that *AtMfl1* is indeed expressed in wt Col leaves and that its expression is enhanced under Fe excess (Fig. 2A).

To analyze the physiological role of *AtMfl1* gene in Fe trafficking, two independent homozygous *Arabidopsis* insertional mutants carrying, respectively, a T-DNA insertion at −154 or −63 bp upstream the starting ATG (+1) in *AtMfl1* promoter (Fig. 2B) were isolated. These mutants, named *atmfl1-1* and *atmfl1-2*, are KO for *AtMfl1* since its expression is completely suppressed in their leaves, in both conditions tested (Fig. 2A). As expected [43,44], expression of the iron storage ferritin *AtFer1* isoform is dependent on Fe supply and indeed *AtFer1* transcript accumulates under Fe excess (Fig. 2A); in such conditions, *AtFer1* transcript accumulation is reduced in *atmfl1* mutants (Fig. 2A), as also shown by quantitative real-time RT-PCR (Fig. 2C).

Wild type Col seedlings, as well as *atmfl1-1* and *atmfl1-2* ones, were grown in conditions of Fe deficiency, sufficiency or excess, by allowing seeds to germinate on AIS plates prepared with either 0, 50 or 500 μM Fe(III)–EDTA. During germination, in conditions of Fe deficiency, *atmfl1-1* and *atmfl1-2* seedlings contain, respectively, 53% and 77% less total Fe than wt seedlings (Fig. 3A). As expected, by increasing Fe availability, i.e., when seedlings were grown on 500 μM Fe(III)–EDTA, total Fe content increases in wt seedlings as well as in *atmfl1-1* and *atmfl1-2* (Fig. 3A). However, in *atmfl1* seedlings, such increase is much lower than in wt, with the total Fe content of *atmfl1-1* and *atmfl1-2* being 40% and 52% lower than wt, respectively (Fig. 3A).

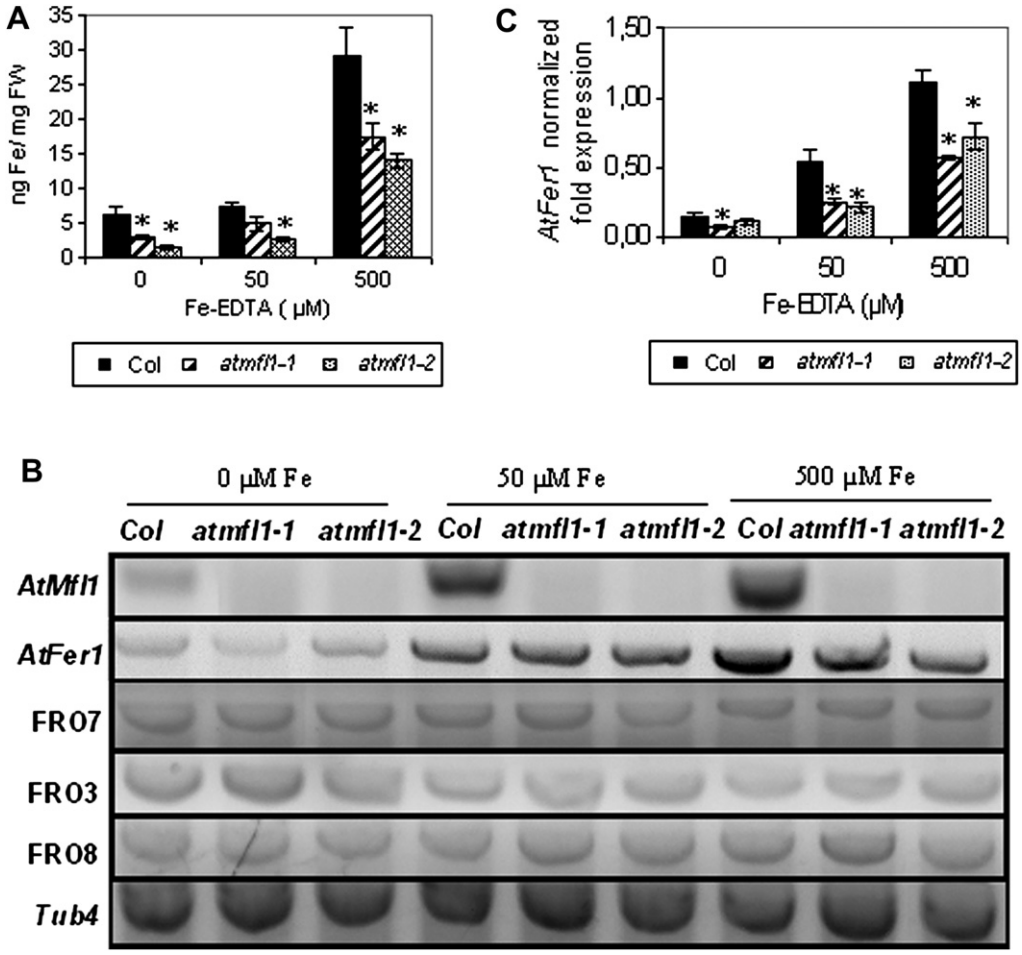

Fig. 3. Characterisation of *atmfl1-1* and *atmfl1-2* seedlings. (A) Col, *atmfl1-1*, *atmfl1-2* seeds germinated in AIS medium containing 0, 50 or 500 µM Fe(III)–EDTA; each bar is the mean total Fe content (ng Fe/mg FW) ±SE of 5 independent samples, measured in 6 d old seedlings. *, $P < 0{,}01$ Student's *t* test (B) RT-PCR analysis of *AtMfl1*, *AtFer1*, FRO7, FRO3, FRO8 transcripts in 6 d old wt Col, *atmfl1-1* and *atmfl1-2* seedlings, germinated as indicated in (A). *Tub4* is the positive control, for testing the equal addition of RNA in each sample. (C) Quantitative real-time RT-PCR on *AtFer1* transcript; the normalized fold expression was detected in cDNA from 6 d old wt Col, *atmfl1-1* and *atmfl1-2* seedlings, germinated as indicated in (A). Bars represent mean values ± SE of three replicates.

As already observed in rosette leaves (Fig. 2A), *AtMfl1* is clearly expressed also in seedlings under Fe sufficiency and such expression is stronger under Fe excess (Fig. 3B) being, on the contrary, weak under Fe deficiency (Fig. 3B). No *AtMfl1* expression was detected in *atmfl1* seedlings in any of the three conditions tested (Fig. 3B).

Under Fe excess, *AtFer1* expression is reduced in *atmfl1* seedlings when compared to wt ones (Fig. 3B) as also shown by quantitative real-time RT-PCR (Fig. 3C). Samples in Figs. 2 and 3 have all been collected at the beginning of the day, that is when *AtMfl1* expression peaks (D. Tarantino, preliminary unpublished observations). The reduction of *AtFer1* expression in *atmfl1* mutants compared to wt is, however, even stronger when seedlings are sampled at midday (Fig. S2), i.e., when the circadian-regulated *AtFer1* expression peaks [31,45].

Expression of the chloroplast FRO7 as well as of the mitochondrial FRO3 or FRO8 were not altered in *atmfl1* mutants, when compared to wt, in any of the different Fe concentrations tested (Fig. 3B). Indeed Pearson's correlation coefficient of *AtMfl1* with FRO7, FRO3 and FRO8 is weak, being respectively 0.52, −0.20 and 0.42 in the log space (Fig. S1).

Rosettes of 21 d *atmfl1-1* and *atmfl1-2* plants are smaller in size, when grown in control conditions (Fig. 4A) or under constant Fe supplement (Fig. 4B): mutant leaves, in both conditions, are significantly shorter (Fig. 4C) and lighter (Fig. 4D) than wt ones. Such differences between mutant and wt plants have been also observed at later growth stages (Fig. S3). When plants are grown under constant Fe supplement, maximal photochemical efficiency is also slightly reduced in *atmfl1* mutants when compared to wt (Fig. 5A) regardless of their unaltered total chlorophyll content (Fig. 5B). Under '+Fe' growth condition, total Fe content is reduced in *atmfl1* leaves as compared to wt one (Fig. 5C).

atmfl1 plants produce the same seed yield as wt plants (Fig. S4A); also, mutant seeds are the same weight (Table S2) and shape (Fig. S4B) as wt, under normal growth but also under constant Fe supplement.

Fe content in embryos from seeds of control grown *atmfl1* plants is similar to wt, since no differences could be detected by Perls stain for Fe (Fig. 6A; Fig. S5A). When grown under constant Fe supplement, Perls stain for Fe is however slightly less intense in *atmfl1* embryos than in wt (Fig. 6B; Fig. S5B), thus suggesting a slight reduction of Fe content in *atmfl1* embryos.

The slight differences of Fe content measured in seeds produced from *atmfl1* and wt plants grown under constant Fe supplement were, however, not statistically significant (Fig. S4C).

3. Discussion

Although essential, the processes of Fe transport into chloroplasts and plant mitochondria are partially unknown; for this reason, we searched for Fe transporters into plant mitochondria.

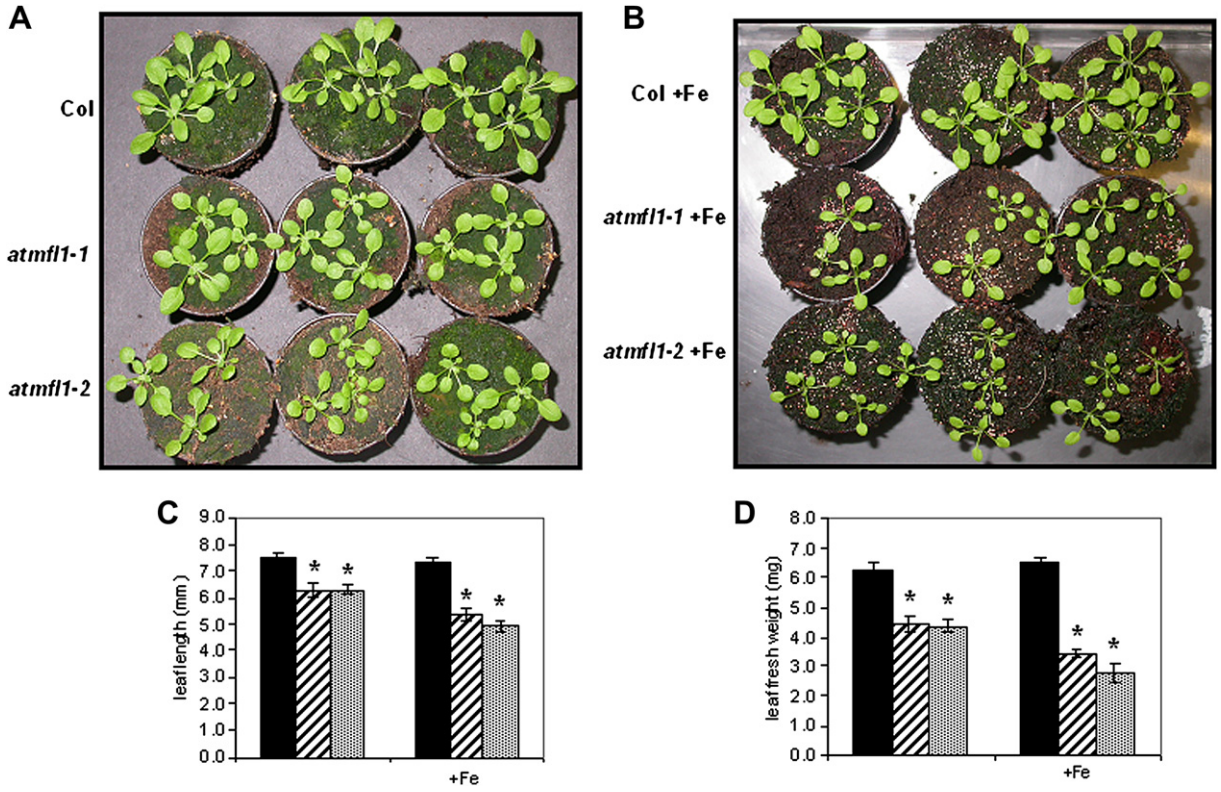

Fig. 4. Characterization of *atmfl1-1* and *atmfl1-2* plants. 21 d old Col, *atmfl1-1*, *atmfl1-2* plants grown in (A) control condition or (B) under constant 2.15 mM Fe(III) supplement; (C) Mean length ± SE of the fourth leaves in 21 d old rosettes of wt Col, *atmfl1-1* and *atmfl1-2* plants, grown in control conditions or under constant, 2.15 mM Fe(III) supplement. 10 rosettes have been sampled for each given value. *, $P < 0{,}01$ Student's *t*-test. (D) Mean weight ± SE for the fourth leaves in 21 d old rosettes of wt Col, *atmfl1-1* and *atmfl1-2* plants grown as in (C). 10 rosettes have been sampled for each given value *, $P < 0{,}01$ Student's *t*-test.

We focused our analysis on a member of the *Arabidopsis* mitochondrial carrier protein family, which we named Mitoferrinlike1 *AtMfl1*, due to its similarity with *D. rerio* MFRN2 Mitoferrin2 [19,20].

In fact, expression of the gene *AtMfl1* (At5g42130) coding for AtMFL1 positively and strongly correlates with genes coding for chloroplast proteins. Also, AtMFL1 is a protein belonging to the chloroplast inner membrane proteome [34,35] as well as AtMFL1 homologs in pea, maize and *B. oleracea* (cauliflower) [37–39]. On the contrary, AtMFL1 was not retrieved in any of the mitochondrial proteome analyses publicly available so far. Taken together, these results are strongly supportive of AtMFL1 localization in chloroplasts only, not in mitochondria.

AtMfl1 is not an essential gene, since two independent *Arabidopsis* KO mutants *atmfl1-1* and *atmfl1-2*, are viable and fertile, though smaller in rosette size. We report three different evidences supporting the hypothesis that *Arabidopsis* AtMFL1 is truly involved in chloroplastic Fe trafficking: (a) *AtMfl1* expression is dependent on Fe supply; (b) total Fe content is reduced in *atmfl1* seedlings and leaves; (c) expression of the iron storage ferritin *AtFer1* is reduced in *atmfl1* seedlings as well as in *atmfl1* leaves, when grown under Fe excess.

Inward-directed ferrous ion transport across chloroplast inner envelope membranes, occurring by a potential-stimulated uniport mechanisms, has been documented [46]. The fact that this transport has saturation kinetics suggested that Fe(II) transport is mediated by a transport protein which could, possibly, facilitate both Fe(II) transport into chloroplast in the light and its release from chloroplast in the dark [46]. This last hypothesis is particularly interesting: AtMFL1, though not essential, could be involved in chloroplast Fe(II) influx or efflux, in order to adjust Fe fluxes to chloroplasts requirements, upon different conditions of Fe supply.

A chloroplast retrograde signal is most probably responsible for regulation of *AtFer1* expression under Fe excess; this signal is, directly or indirectly, dependent on the nitric oxide burst observed in *Arabidopsis* chloroplasts soon after cell treatment with Fe excess [44,47].

The reduced *AtFer1* expression in *atmfl1* seedlings and plants grown under constant Fe supplement also supports the hypothesis that a signal from the chloroplast to the nucleus informs about perturbation of chloroplast Fe homeostasis which, in turn, triggers activation of a particular sets of genes, among which ferritin *AtFer1*; such retrograde signalling should sense also the perturbation in chloroplast Fe transport into chloroplasts, as it possibly occurs in *atmfl1* mutants.

According to this hypothesis, several events should occur in *atmfl1* mutants, such as alteration in chloroplast Fe content and in the extent of the nitric oxide burst as well as abnormal accumulation of the intermediates of tetrapyrrole synthesis; testing this hypothesis will be focus of our future research.

4. Materials and methods

4.1. Plant material

Arabidopsis plants were grown as in [48] and constantly irrigated with either tap water (controls) or 2.15 mM Fe(III) (from Fe (III)–EDDHA, containing 6% Fe(III) (w:w) in the Fe chelate).

4.2. Seedlings growth

Seeds (at least 60 seeds/plate) were germinated on square plates (10 cm × 10 cm) containing AIS medium [48] at pH 6.0 (with

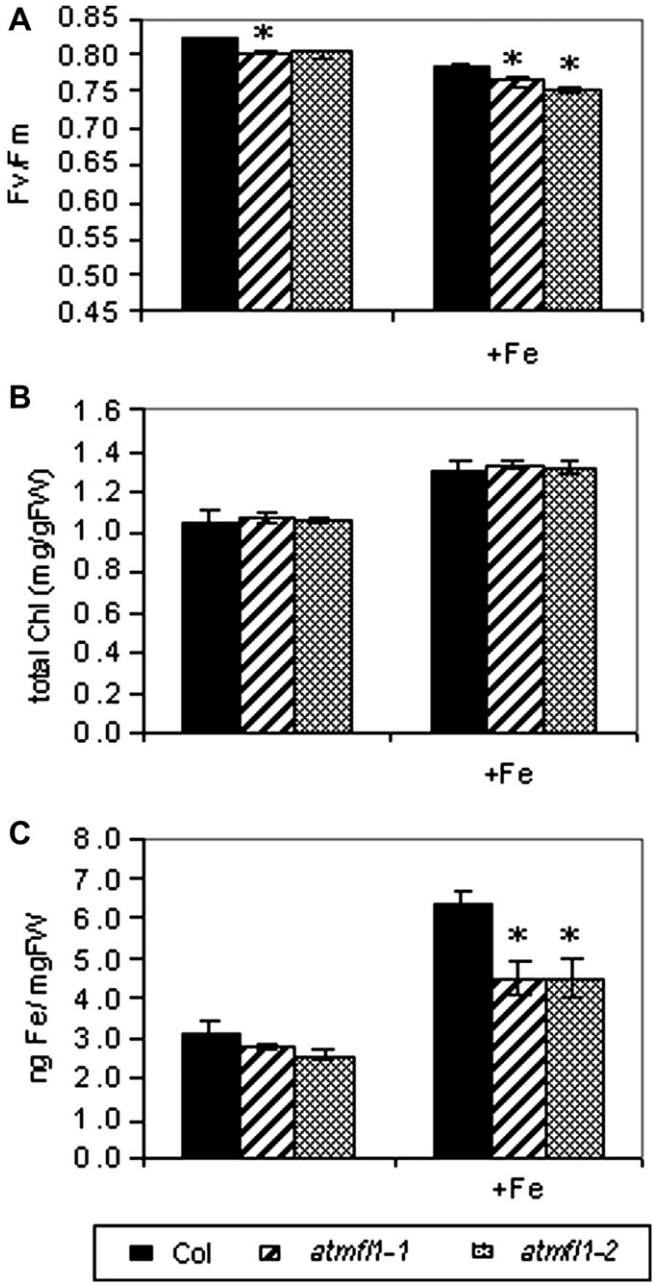

Fig. 5. Characterisation of *atmfl1-1* and *atmfl1-2* plant grown in control conditions or under constant, 2.15 mM Fe(III) supplement (A) maximal photochemical efficiency parameter Fv/Fm; (B) total chlorophyll content (chlorophyll *a* + chlorophyll *b*), expressed as mg Chl/g FW; (C) leaf iron content, expressed as ng Fe/mg FW. Bars in (A) represent mean value ± SE of 10 independent samples, bars in (B,C) represent mean value ± SE of 5 independent samples. *, $P < 0{,}01$ Student's *t*-test.

BTP): iron content of the AIS medium was either 0, 50 or 500 μM Fe (III)–EDTA (Fe-deficient, -sufficient or excess condition, respectively). Plate were kept upward, in the greenhouse, at 25 °C, 100 μmol photons/m^2 sec, 14 h light/10 h dark period (from 6:00 a.m. to 20:00 p.m.) unless otherwise specified. Sampling started 6 d after germination.

4.3. Isolation of atmfl1-1 and atmfl1-2 mutants

N556579 and N507617 heterozygous mutant lines (Salk collection of *Arabidopsis* T-DNA insertional mutants) have the T-DNA inserted at −154 and −63 bp in the *AtMfl1* gene promoter, respectively. Each line was selfed and progeny plants were tested for the presence of T-DNA in *AtMfl1* gene promoter by PCR reactions, using a primer specific for the T-DNA Left Border:

LBa1 5′-TGGTTCACGTAGTGGGCCATCG-3′ and primers specific for *AtMfl1* gene:
MFL1for: 5′- AAATGGTTAGCCAACTTCATGCCG-3′
MFL1rev: 5′-TTCTGACGATAGGGCTTTGGACG -3′. (65 °C anneal.-temp., 2 mM $MgCl_2$).

Progeny plants of N556579 and N507617 lines, homozygous for the T-DNA insertion, were named *atmfl1-1* and *atmfl1-2* respectively and were propagated for their characterization.

4.4. Evaluation of leaf weight and length

For measuring leaf length and weight, rosette leaf nr. 4 (nr.1 being the youngest true rosette leaf) from either 21 or 30 d old rosettes were sampled, weighed and their length measured (excluding petiole).

4.5. RT-PCR

Total RNA was extracted from seedlings with Trizol® reagent (Gibco); 1 μg RNA was retro-transcribed to cDNA in 10 μl final volume by using the DyNAmo cDNA Synthesis kit (Finnzymes, Finland), following the manufacturer's instruction. After a cDNA dilution (dilution factor is reaction-specific) according to the primer in nuclease-free water, 1 μl cDNA was used as template for each PCR reaction. For amplification of *AtMfl1* cDNA fragment (At5g42130) the following primer pair was used:

Mfl1for: 5′-ATGGAAGCTAGACTCTCCG-3′
Mfl1rev: 5′-TCAAGAATCAGCAGCAACG-3′(674 bp fragment size, 65 °C annealing temp., 2 mM $MgCl_2$,cDNA dilution 1:1).

For amplification of *AtFer1* cDNA fragment (At5g01600) the following primer pair was used:

Fer1for: 5′-TAAGCCACTACTCCCTCACG-3′
Fer1rev: 5′-TTTGTGAACGTTTAGAAGCTTCTC-3′ (574 bp fragment size, 63 °C anneal.temp., 2 mM $MgCl_2$, cDNA dilution 1:20).

For amplification of FRO3 cDNA fragment (At1g23020) the following primer pair was used:

FRO3for:5′-TTCAATAGCAGTAAGGTTAGG-3′
FRO3rev:3′-AAGCTCGACAGTTTCACAAGG-3′ (526 bp fragment size, 60 °C anneal.temp., 2.5 mM $MgCl_2$, cDNA dilution 1:10).

For amplification of FRO7 cDNA fragment (At5g49740) the following primer pair was used:

FRO7for:5′-TTCGAGCATGCTACAAGATACC-3′
FRO7rev:3′-TTACGGTGTAGGATATCGC-3′ (806 bp fragment size, 60 °C anneal.temp., 2.5 mM $MgCl_2$, cDNA not diluted).

For amplification of FRO8 cDNA fragment (At5g50160) the following primer pair was used:

FRO8for:5′-AAGTACTATAGAGTTGCTACAAGG-3′
FRO8rev:3′-GATTGGCGGAAAGAATGCAGC-3′ (511 bp fragment size, 60 °C anneal.temp., 2.5 mM $MgCl_2$, cDNA dilution 1:10).

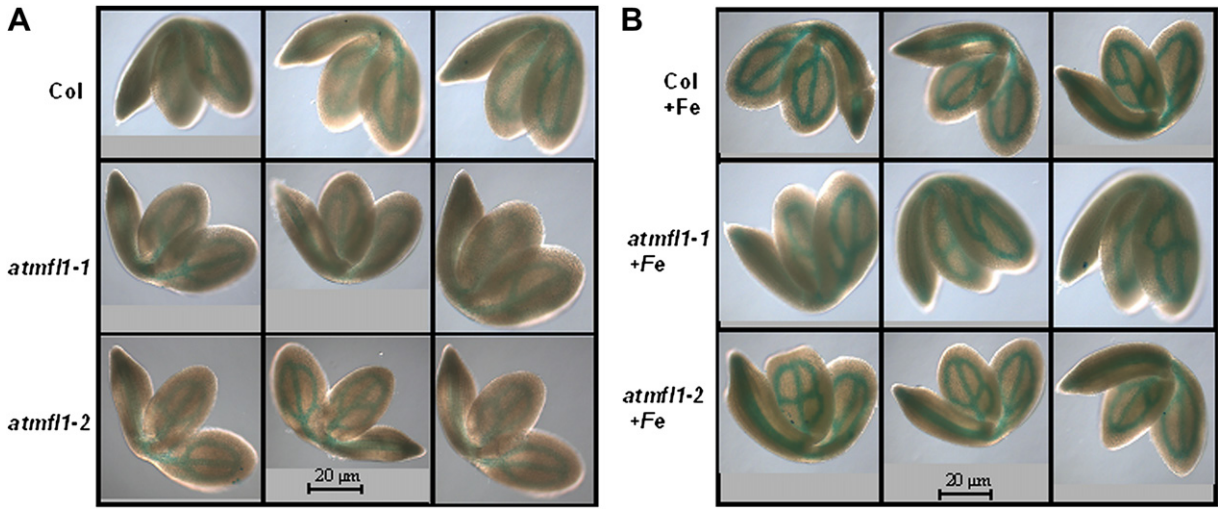

Fig. 6. Characterization of Col, *atmfl1-1*, *atmfl1-2* mature embryos. Seeds were collected from Col, *atmfl1-1*, *atmfl1-2* plants grown either in control condition or under constant 2.15 mM Fe(III) supplement; (A) Fe detection, using Perls stain giving a blue colour, in Col, *atmfl1-1* and *atmfl1-2* embryos from plants grown in control condition. (B) Fe detection, using Perls stain, in Col, *atmfl1-1* and *atmfl1-2* embryos from plants grown under constant Fe supplement. Bars in (A) and (B) correspond to 20 µm.

For amplification of *AtTub4* cDNA fragment (At5g44340) the following primer pair was used:

Tub4for: 5′-AGAGGTTGACGAGCAGATGA-3′
Tub4rev: 5′-CCTCTTCTTCCTCCTCGTAC-3′ (350 bp fragment size, 60 °C anneal.temp., 2.5 mM $MgCl_2$, cDNA dilution 1:20).

4.6. Quantitative real-time RT-PCR

AtFer1 transcript enrichment fold was detected using a Sybr Green Assay (Bio-Rad, http://www.bio-rad.com/) with the reference gene Ubiquitin. The real-time PCR assay was conducted in triplicate and was performed in Bio-Rad C1000 Thermal Cycler optical system. Relative enrichment of *AtFer1* transcript was calculated normalizing the amount of mRNA against an Ubiquitin fragment. Diluted aliquots of the reverse-transcribed cDNAs were used as templates in quantitative PCR reactions containing the Sybr Green Supermix (Bio-Rad). The difference between the cycle threshold (Ct) of *AtFer1* and the Ct of Ubiquitin was used to obtain the normalized expression of *AtFer1*. Relative enrichments were calculated as previously described [49]. The expression of *AtFer1* was analysed by using the following primer pair:

Fer1RTfor1: 5′-ACTCCACCCTATCGTCTCACC-3′
Fer1rev:5′-TTTGTGAACGTTTAGAAGCTTCTC-3′

The expression of the reference gene Ubiquitin was analysed by using the following primer pair:

UBI for: 5′-CTGTTCACGGAACCCAATTC-3′
UBI rev: 5′-GGAAAAAGGTCTGACCGACA-3′

4.7. Iron quantification and staining

Seedlings and leaves were weighed fresh and frozen in liquid nitrogen. Total iron quantification was then performed as indicated in [48]. For the Pearls stain for iron, the protocol in [50] was applied; briefly: mature seeds were imbibed for 3 h in distilled water and embryos were dissected under a binocular microscope. The isolated embryos were vacuum infiltrated 2 min with Perls stain solution (4% HCl, 4% potassium-ferrocyanide 1:1), then left in the solution for 15 min at room temperature in the dark and washed three times (5 min each wash) with distilled water by gentle shaking. Embryos were analysed with an optical microscope and images were captured with AxiocamMRc5 camera (Zeiss) using the Axiovision program (version 4.1).

4.8. Chlorophyll quantification and Fv/Fm measurements

Total chlorophyll content and maximal photochemical efficiency parameter Fv/Fm measurements were performed according to [43].

4.9. Analysis of sequence homology

Protein sequence homology analysis was performed with BLASTP program, on TAIR9 *Arabidopsis* protein dataset, at http://www.arabidopsis.org/Blast/index.jsp. Sequence alignment was performed with ClustalW2 at: http://www.ebi.ac.uk/Tools/clustalw2/index.html.

4.10. Prediction of mitochondrial localization

Analysis was performed by using the Aramemnon database at:

http://aramemnon.botanik.uni-koeln.de.

4.11. Prediction of transmembrane regions and orientation

Prediction was performed by using the following programs:

TMpred at http://www.ch.embnet.org/software/TMPRED_form.html
TMHMM Server v. 2.0 at http://www.cbs.dtu.dk/services/TMHMM/.

4.12. Expression correlation analysis

The calculation of the Pearson's correlation coefficient between expression levels for every gene pair was done by using a dataset of 1750 microarray hybridizations as described in [30,51]. Calculations

have been performed on the expression values as such, or after logarithmic transformation.

Acknowledgements

N556579 and N507617 heterozygous mutant seeds were kindly provided by TAIR (The Arabidopsis Information Resource, http://www.arabidopsis.org/). We thank Riccardo Pacella for help during the first experiments and Francesca Resentini for assistance during quantitative RT-PCR experiments. We are grateful to Prof. Robert Jennings for kindly revising manuscript text. This work was supported by MIUR (PRIN 2008, prot. Nr. 20084XTFBC).

Appendix. Supplementary data

Supplementary data associated with this article can be found in the online version, at doi:10.1016/j.plaphy.2011.02.003.

References

[1] S.A. Kim, M.L. Guerinot, Mining iron: iron uptake and transport in plants, FEBS Lett. 581 (2007) 2273–2280.
[2] J. Balk, S. Lobreaux, Biogenesis of iron-sulfur proteins in plants, Trends Plant Sci. 10 (2005) 324–331.
[3] I. Lermontova, E. Kruse, H.P. Mock, B. Grimm, Cloning and characterization of a plastidial and a mitochondrial isoform of tabacco protoporphyrinogen IX oxidase, Proc. Natl. Acad. Sci. 94 (1997) 8895–8900.
[4] S. Mackenzie, L. McIntosh, Higher plant mitochondria, Plant Cell 11 (1999) 571–585.
[5] W. Frank, K.M. Baar, E. Qudeimat, M. Woriedh, A. Alawady, D. Ratnadewi, L. Gremillon, B. Grimm, R. Reski, A mitochondrial protein homologous to the mammalian peripheral-type benzodiazepine receptor is essential for stress adaptation in plants, Plant J. 51 (2007) 1004–1018.
[6] R. Tanaka, A. Tanaka, Tetrapyrrole biosynthesis in higher plants, Annu. Rev. Plant Biol. 58 (2007) 321–346.
[7] N. Bughio, M. Takahashi, E. Yoshimura, N.K. Nishizawa, S. Mori, Light-dependent iron transport into isolated barley chloroplasts, Plant Cell Physiol. 38 (1997) 101–105.
[8] D. Duy, G. Wanner, A.R. Meda, N. von Wiren, J. Soll, K. Philippar, PIC1, an ancient permease in *Arabidopsis* chloroplasts, mediates iron transport, Plant Cell 19 (2007) 986–1006.
[9] Y.S. Teng, Y.S. Su, L.Y. Chen, Y.J. Lee, I. Hwang, H. Li, Tic21 is an essential translocon component for protein translocation across the chloroplast inner envelope membrane, Plant Cell 18 (2006) 2247–2257.
[10] S. Kikuchi, M. Oishi, Y. Hirabayashi, D.W. Lee, I. Hwang, M. Nakai, A 1-Megadalton translocon complex containing Tic20 and Tic21 mediates chloroplasts protein import at the inner envelope membrane, Plant Cell 21 (2009) 1781–1797.
[11] I. Mukherjee, N.H. Campbell, J.S. Ash, E.L. Connolly, Expression profiling of the *Arabidopsis* ferric chelate reductase (FRO) gene family reveals differential regulation by iron and copper, Planta 223 (2006) 1178–1190.
[12] J. Jeong, E.L. Connolly, Iron uptake mechanisms in plants: functions of the FRO family of ferric reductases, Plant Sci. 176 (2009) 709–714.
[13] J. Jeong, M.L. Guerinot, Homing in on iron homeostasis in plants, Trends Plant Sci. 14 (2009) 280–285.
[14] C. Curie, J.F. Briat, Iron transport and signalling in plants, Annu. Rev. Plant Biol. 54 (2003) 183–206.
[15] J. Jeong, C. Cohu, L. Kekeb, M. Pilon, E.L. Connolly, M.L. Guerinot, Chloroplast Fe (III) chelate reductase activity is essential for seedling viability under iron limiting conditions, Proc. Natl. Acad. Sci. 105 (2008) 10619–10624.
[16] D. Tarantino, N. Santo, P. Morandini, F. Casagrande, H.P. Braun, J. Heinemeyer, G. Vigani, C. Soave, I. Murgia, AtFer4 ferritin is a determinant of iron homeostasis in *Arabidopsis thaliana* heterotrophic cells, J. Plant. Physiol. 167 (2010) 1598–1605.
[17] S. Kushnir, E. Babiychuck, S. Storozhenko, M.W. Davey, J. Papenbrock, R. De Rycke, G. Engler, U.W. Stephan, H. Lange, G. Kispal, A mutation in the mitochondrial ABC transporter Sta1 leads to dwarfism and chlorosis in the *Arabidopsis* mutant starik1, Plant Cell 13 (2001) 89–100.
[18] D.Y. Kim, L. Bovet, S. Kushnir, E.W. Noh, E. Martinoia, Y. Lee, AtATM3 is involved in heavy metal resistance in *Arabidopsis*, Plant Physiol. 140 (2006) 922–932.
[19] G.C. Shaw, J.J. Cope, L. Li, K. Corson, C. Hersey, G.E. Ackermann, B. Gwynn, A.J. Lambert, R.A. Wingert, D. Traver, N.S. Trede, B.A. Barut, Y. Zhou, E. Minet, A. Donovan, A. Brownlie, R. Balzan, M.J. Weiss, L. Peters, J. Kaplan, L.I. Zon, B.H. Paw, Mitoferrin is essential for erythroid iron assimilation, Nature 440 (2006) 96–100.
[20] P.N. Paradkar, K.B. Zumbrennen, B.H. Paw, D.M. Ward, J. Kaplan, Regulation of mitochondrial iron import through differential turnover of mitoferrin 1 and mitoferrin 2, Mol. Cell. Biol. 29 (2009) 1007–1016.
[21] N. Picault, M. Hodges, L. Palmieri, F. Palmieri, The growing family of mitochondrial carrriers in *Arabidopsis*, Trends Plant Sci. 9 (2004) 138–146.
[22] A.H. Millar, J.L. Heazlewood, Genomic and proteomic analysis of mitochondrial carrier proteins in *Arabidopsis*, Plant Physiol. 131 (2003) 443–453.
[23] L. Palmieri, R. Arrigoni, E. Blanco, F. Carrari, M.I. Zanor, C. Studart-Guimaraes, A.R. Fernie, F. Palmieri, Molecular identification of an *Arabidopsis* S-adenosylmethionine transporter. Analysis of organ distribution, bacterial expression, reconstitution into liposomes and functional characterization, Plant Physiol. 142 (2006) 855–865.
[24] F. Bouvier, N. Linka, J.C. Isner, J. Mutterer, A.P.M. Weber, B. Camara, *Arabidopsis* SAMT1 defines a plastid transporter regulating plastid biogenesis and plant development, Plant Cell 18 (2006) 3088–3105.
[25] I. Haferkamp, The diverse members of the mitochondrial carrier family in plants, FEBS Lett. 581 (2007) 2375–2379.
[26] F. Palmieri, Mitochondrial carrier proteins, FEBS Lett. 346 (1994) 48–54.
[27] R. Månsson, P. Tsapogas, M. Akerlund, A. Lagergren, R. Gisler, M. Sigvardsson, Pearson correlation analysis of microarray data allows for the identification of genetic targets for early B-cell factor, J. Biol. Chem. 279 (2004) 17905–17913.
[28] T. Gigolashvili, R. Yatusevich, I. Rollwitz, M. Humphry, J. Gershenzon, U.I. Flügge, The plastidic bile acid transporter 5 is required for the biosynthesis of methionine-derived glucosinolates in *Arabidopsis thaliana*, Plant Cell (2009) 1813–1829.
[29] K. Vandepoele, M. Quimbaya, T. Casneuf, L. De Veylder, Y. Van de Peer, Unraveling transcriptional control in *Arabidopsis* using cis-regulatory elements and co-expression networks, Plant Physiol. (2009) 535–546.
[30] M. Menges, R. Dóczi, L. Okrész, P. Morandini, L. Mizzi, M. Soloviev, J.A. Murray, L. Bögre, Comprehensive gene expression atlas for the *Arabidopsis* MAP kinase signalling pathways, New Phytol. 179 (2008) 643–662.
[31] I. Murgia, D. Tarantino, C. Soave, P. Morandini, The Arabidopsis CYP82C4 expression is dependent on Fe availability and the circadian rhythm and it correlates with genes involved in the early Fe-deficiency response, J. Plant Physiol. (2011). doi:10.1016/j.jplph.2010.11.020.
[32] T. Kleffmann, D. Russenberger, A. Zychlinski, A. Christopher, K. Sjolander, W. Gruissem, S. Baginsky, The *Arabidopsis thaliana* chloroplast proteome reveals pathway abundance and novel protein functions, Curr. Biol. 14 (2004) 354–362.
[33] M. Ferro, D. Salvi, S. Brugiere, S. Miras, S. Kowalski, M. Louwagie, J. Garin, J. Joyard, N. Rolland, Proteomics of the chloroplasts envelope membranes from *Arabidopsis thaliana*, Mol. Cell. Proteomics 2 (2003) 325–345.
[34] B. Zybailov, H. Rutschow, G. Friso, A. Rudella, O. Emanuelsson, Q. Sun, K.J. van Wijk, Sorting signals, N-Terminal modifications and abundance of the chloroplast proteome, PloS One 3 (2008) e1994.
[35] Q. Sun, B. Zybailov, W. Majeran, G. Friso, P.D. Olinares, K.J. van Wijk, PPDB, the plant proteomics database at cornell, Nucleic Acids Res. 37 (2009) D969–D974.
[36] M. Ferro, S. Brugiére, D. Salvi, D. Seigneurin-Berny, M. Court, L. Moyet, C. Ramus, S. Miras, M. Mella, S. Le Gall, S. Kieffer-Jaquinod, C. Bruley, J. Garin, J. Joyard, C. Masselon, N. Rolland, AT-CHLORO, a comprehensive chloroplast proteome database with subplastidial localization and curated information on envelope proteins, Mol. Cell. Proteomics 9 (2010) 1063–1084.
[37] A. Bräutigam, S. Hoffmann-Benning, A.P.M. Weber, Comparative proteomics of chloroplast envelopes from C3 and C4 plants reveals specific adaptations of the plastid envelope to C4 photosynthesis and candidate proteins required for maintaining C4 metabolite fluxes, Plant Physiol. 148 (2008) 568–579.
[38] A. Bräutigam, R.P. Shrestha, D. Whitten, C.G. Wilkerson, K.M. Carr, J.E. Froehlich, A.P.M. Weber, Low-coverage massively parallel pyrosequencing of cDNAs enables proteomics in non-model species: comparison of the use of a species-specific database generated by prosequencing with databases from related species from proteome analysis of pea chloroplast envelopes, J. Biotechnol. 136 (2008) 44–53.
[39] A. Bräutigam, A.P.M. Weber, Proteomic analysis of the proplastid envelope membrane provides novel insights into small molecule and protein transport across proplastid membranes, Mol. Plant 2 (2009) 1247–1261.
[40] J.B. Peltier, G. Friso, D.E. Kalume, P. Roepstorff, F. Nilsson, I. Adamska, K.J. Van Wijk, Proteomics of the chloroplast: systematic identification and targeting analysis of lumenal and peripheral thylakoid proteins, Plant Cell 12 (2000) 319–341.
[41] V. Kruft, H. Eubel, L. Jänsch, W. Werhahn, H.P. Braun, Proteomic approach to identify novel mitochondrial proteins in *Arabidopsis*, Plant Physiol. 127 (2001) 1694–1710.
[42] D. Winter, B. Vinegar, H. Nahal, R. Ammar, G.V. Wilson, N.J. Provart, An "Electronic fluorescent pictograph" browser for exploring and analyzing large-scale biological data sets, PLoS One 2 (2007) e718.
[43] I. Murgia, V. Vazzola, D. Tarantino, F. Cellier, K. Ravet, J.F. Briat, C. Soave, Knock-out of ferritin *AtFer1* causes earlier onset of age-dependent leaf senescence in *Arabidopsis*, Plant Physiol. Biochem. 45 (2007) 898–907.
[44] J.F. Briat, N. Arnaud, C. Duc, J. Boucherez, B. Touraine, F. Cellier, F. Gaymard, New insights into ferritin synthesis and function highlight a link between iron homeostasis and oxidative stress in plants, Ann. Bot. 105 (2010) 811–822.
[45] C. Duc, F. Cellier, S. Lobreaux, J.F. Briat, F. Gaymard, Regulation of iron homeostasis in *Arabidopsis thaliana* by the clock regulator time for coffee, J. Biol. Chem. 284 (2009) 36271–36281.

[46] R. Shingles, M. Noth, R.E. McCarty, Ferrous ion transport across chloroplast inner envelope membranes, Plant Physiol. 128 (2002) 1022–1030.
[47] N. Arnaud, I. Murgia, J. Boucherez, J.F. Briat, F. Cellier, F. Gaymard, An iron-induced nitric oxide burst precedes ubiquitin-dependent protein degradation for *Arabidopsis AtFer1* ferritin gene expression, J. Biol. Chem. 281 (2006) 23579–23588.
[48] D. Tarantino, F. Casagrande, C. Soave, I. Murgia, Knocking out of the mitochondrial *AtFer4* ferritin does not alter response of *Arabidopsis* plants to abiotic stresses, J. Plant. Physiol. 167 (2010) 453–460.
[49] V. Gregis, A. Sessa, L. Colombo, M.M. Kater, AGAMOUS-LIKE24 and SHORT VEGETATIVE PHASE determine floral meristem identity in *Arabidopsis*, Plant J. 56 (2008) 891–902.
[50] H. Roschzattardtz, G. Conéjéro, C. Curie, S. Mari, Identification of the endodermal vacuole as the iron storage compartment in the *Arabidopsis* embryo, Plant Physiol. 151 (2009) 1329–1338.
[51] M. Menges, G. Pavesi, P. Morandini, L. Bögre, J.A. Murray, Genomic organization and evolutionary conservation of plant D-type cyclins, Plant Physiol. 145 (2007) 1558–1576.